The Compact Muon Solenoid Experiment

Conference Report

Mailing address: CMS CERN, CH-1211 GENEVA 23, Switzerland

Time Alignment of the CMS Hadron Calorimeter

Gillian Kopp, Chris Tully, Wonyong Chung, Kiley Kennedy, Svitlana Hoienko, Jeremy Mans, Michael Krohn, Bryan Crossman, Joshua Hiltbrand, Andris Skuja, Long Wang

Abstract

The Hadron Calorimeter (HCAL) in the Compact Muon Solenoid (CMS) experiment at the Large Hadron Collider (LHC) was recently upgraded for Run 3 (2022-2025) to introduce depth segmentation and online timing measurements. With increased segmentation and readout channels, the HCAL provides new timing capabilities for jets and hadronic tau decays with nearly 4π coverage and sensitivity to highly displaced decays within the calorimeter volume. Recent HCAL timing scans provide a valuable look at artificially delayed jets in collision data and are crucial to improving the detectors performance. Online timing is utilized for detector alignment based on positioning the pulse rising edge, achieving an alignment accuracy of 0.5 ns, considerably higher than previous energy-weighting based approaches. Using precision arrival time measurements, significant advances have been made in understanding the propagation of hadronic showers throughout the calorimeter.

Presented at *CALOR2024 20th International Conference on Calorimetry in Particle Physics*

Time Alignment of the CMS Hadron Calorimeter

Gillian Kopp[1,*], *Chris* Tully[1], *Wonyong* Chung[1], *Kiley* Kennedy[1], *Svitlana* Hoienko[1], *Jeremy* Mans[2], *Michael* Krohn[2], *Bryan* Crossman[2], *Joshua* Hiltbrand[3], *Andris* Skuja[4], and *Long* Wang[4]

[1]Princeton University
[2]University of Minnesota
[3]Baylor University
[4]University of Maryland

Abstract. The Hadron Calorimeter (HCAL) in the Compact Muon Solenoid (CMS) experiment at the Large Hadron Collider (LHC) was recently upgraded for Run 3 (2022-2025) to introduce depth segmentation and online timing measurements. With increased segmentation and readout channels, the HCAL provides new timing capabilities for jets and hadronic tau decays with nearly 4π coverage and sensitivity to highly displaced decays within the calorimeter volume. Recent HCAL timing scans provide a valuable look at artificially delayed jets in collision data and are crucial to improving the detector's performance. Online timing is utilized for detector alignment based on positioning the pulse rising edge, achieving an alignment accuracy of 0.5 ns, considerably higher than previous energy-weighting based approaches. Using precision arrival time measurements, significant advances have been made in understanding the propagation of hadronic showers throughout the calorimeter.

1 Introduction

The Compact Muon Solenoid (CMS) experiment records proton-proton collisions at the Large Hadron Collider (LHC) at CERN near Geneva, Switzerland. The CMS experiment consists of multiple subdetectors providing nearly hermetic coverage, each designed to measure the energy or momentum of particles produced from a primary proton-proton collision. The CMS hadron calorimeter (HCAL) measures the energy of hadrons with four sections: barrel (HB), endcap (HE), outer (HO), and forward (HF). HB and HE are sampling calorimeters made of layers of brass absorber interleaved with plastic scintillator tiles and cover pseudorapidity $|\eta| \leq 1.4$ and $1.3 < |\eta| < 3.0$, respectively. An incident particle undergoes a nuclear interaction in the absorber, and the resulting shower of secondary particles is detected in the scintillation layers. Scintillation light is extracted on wavelength-shifting fibers and subsequently observed on SiPMs (silicon photomultipliers made of Geiger-mode avalanche photodiodes).

In the Phase-1 upgrade in 2018 of the HCAL barrel and endcap, SiPMs replaced hybrid photodiodes to enable a higher photon detection efficiency, better signal-to-noise performance, and increased energy resolution [1]. This upgrade increased the number of readout channels and enabled per-depth readouts, with 4 depths in HB and up to 7 in HE, shown in Figure 1. Additionally, the front-end ASIC (QIE11 chip [2]) was updated to provide both time and energy measurements from each HCAL cell. The QIE11 digitizes the pulse from each readout channel and

performs charge integration and digitization (ADC) along with time-to-digital conversion (TDC) with 0.5 ns granularity. The energy response is reported in 25 ns timeslices, and a consistent arrival time for all pulses across the detector will ensure the best calorimeter energy resolution.
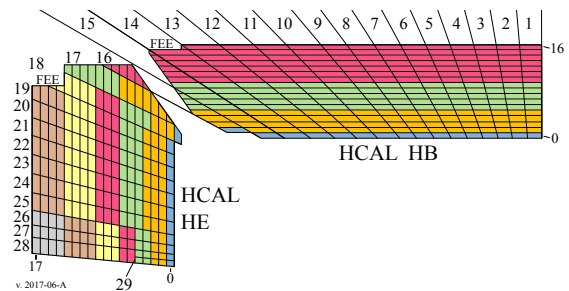

Figure 1. Illustration of the HB and HE, with each color representing a depth layer. Energy and time measurements are available at each cell (per depth, $i\eta$, and $i\phi$). $i\eta$, with a width of $\Delta\eta = 0.087$, refers to the HCAL towers and runs from 1 to 29. HB covers $|16| \leq i\eta$, and HE covers $16 < |i\eta| \leq 29$.

2 HCAL Timing Measurements

The TDC from the QIE11 chip provides high-precision timing information for each HCAL channel. The SiPM current vs. time pulse is compared to a flat current threshold (8-bit programmable value, set at 18.7 μA in Run 3) to determine the TDC value. The time at which the current

---

*e-mail: gillian.baron.kopp@cern.ch

passes this threshold is the TDC value, reported in a 6-bit digital output, with 0.5 ns bins in the 25 ns timeslice.

In HB, a firmware look-up table (LUT) compresses the 6-bit TDC into 2-bits, required due to bandwidth constraints [3]. This 6:2 LUT is defined from per-$i\eta$ and depth "prompt" and "delayed" TDC ranges. The resulting 2-bit compressed TDC encodes four ranges: prompt, slightly delayed, very delayed, and invalid/error. The last value of the prompt range, denoted t_p, and the boundary between the two delayed ranges, denoted t_d, defines the 6:2 LUT.

- 00 = prompt pulse, with TDC $\leq t_p$
- 01 = slightly delayed, with $t_p <$ TDC $\leq t_d$
- 10 = very delayed, with $t_d <$ TDC < 50
- 11 = invalid pulse, with $50 \leq$ TDC

2.1 Time Alignment of the Calorimeter

A new HB TDC-based alignment method is developed and demonstrated to achieve alignment to within 0.5 ns. TDC records the arrival time of the pulse rising edge and is beneficial in detector time alignment, which is vital for the calorimeter's timing and energy measurements.

Data from a timing (or "phase") scan in which the HCAL clock is scanned relative to the LHC clock enables the evaluation of a range of HCAL alignment settings. Phase scans are run during proton-proton collisions, such that the alignment method accounts for both the detector time and energy resolution and the effects of shower propagation through the calorimeter material. For the scans in 2022 and 2023, the TDC LUT is identical for all $i\eta$ and depth values in HB, setting $t_p = 12$, or 6 ns, and $t_d = 14$, or 7 ns (Section 2). This creates three timing ranges: 0-6 ns, 6.5-7 ns, and 7.5-25 ns. An illustration of the four timing ranges and the flat current threshold defining where the TDC is set is shown in Figure 2.
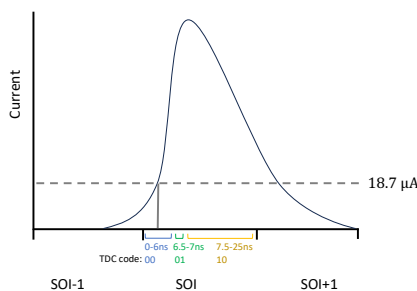

Figure 2. Diagram of the 2-bit TDC code ranges as measured by the rising time of a pulse. The 25 ns timeslice where the triggered event occurs is called the sample of interest (SOI).

Relying on the TDC information for calorimeter time alignment is ideal, as this ensures that the rising edge of the pulse is fully captured and minimizes sensitivity to fluctuations in the tail of the pulse due to developing hadronic showers.

2.2 Timing Scan Analysis

Implementing the TDC-based method achieved HB time alignment within 0.5 ns precision, such that prompt pulses arrive at the detector simultaneously, consistent across depth and $i\eta$. Optimal alignment is achieved when the fraction of prompt TDC codes is maximized. This ensures that the rising edge of the energy response is placed close to the start of the 25 ns timeslice of interest, and avoids spillover into the previous bunch crossing. The TDC-based method presented accounts for shower propagation through each depth and accurately aligns the calorimeter.

The timing scan data is evaluated to set pulse arrival times consistently across HB. A dataset enriched in jets or missing transverse energy is used, and a minimum energy of 4 GeV E_T (to minimize time-slew effects) for a single HCAL cell is required for the pulse to be included in the analysis. For channels with pulses satisfying this requirement, the distribution of TDC codes is plotted, and HCAL phase settings are adjusted (online, as the QIE11 phase) such that arrival time distributions are the same across HB.

Figure 3 shows a typical TDC code distribution during the 2023 HCAL phase scan, with the 0 ns QIE phase offset representing ideal alignment. The analysis is performed for HB ($|i\eta| \leq 16$), and results are consistent across all $i\eta$. The TDC code fraction is the fraction of cells with each TDC code (4 codes) for cells (individual $i\eta, i\phi$, and depth) over 4 GeV E_T. The prompt TDC distribution (blue, TDC ≤ 6 ns) shows the prompt pulse arrival spread and is maximized at an offset of 0 ns. As the phase offset increases, more delayed (green and orange) TDC codes are seen as pulses arrive in the delayed region. The prompt fraction increases as the next bunch crossing enters (phase offset of 20 ns). Ideal alignment places the prompt peak at a phase offset of 0 ns, such that the pulse rising edge is close to the start of the timeslice. This ideal alignment is achieved for all channels in HB to within 0.5 ns, the TDC step size.
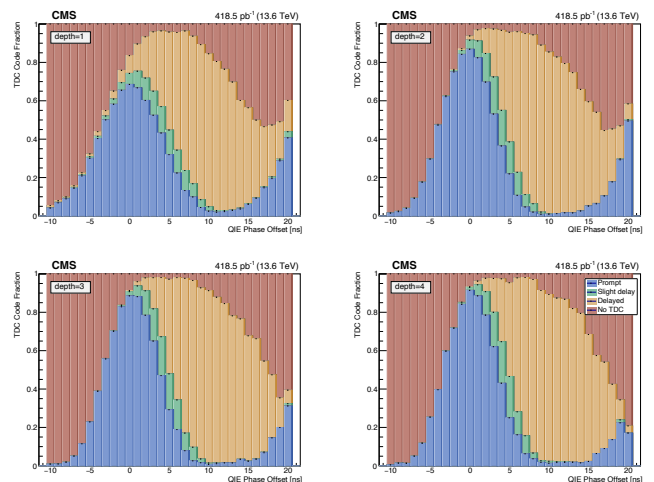

Figure 3. Distribution of TDC codes vs. QIE scan, for each of 4 depths across HB, for $i\eta = -10$ in the SOI, during the May 2023 QIE phase scan. QIE phase offset of 0 ns represents ideal alignment, with the prompt fraction maximized. Published in [4].

There is a Gaussian spread of arrival times of the pulse rising edge within each QIE phase setting, and the distribution of these arrival times is shown in Figure 3 in blue. The prompt window (TDC=00) is kept as narrow as possible. From the phase scan TDC distributions, the prompt fraction drops off rapidly at -2 and -4 ns, indicating that the arrival time distribution is close to the clock boundary. In addition, the prompt distribution does not plateau, indicating that the prompt window is not unnecessarily large.

The TDC threshold is high enough not to fire from pileup (a contribution from additional overlapping proton-proton collisions) in the previous bunch crossing, while other time approximation methods (CWT, discussed in Section 3) will be more susceptible to pileup.

2.3 TDC-based Alignment Improvements

Similar phase scan analysis demonstrated that position-dependent misalignments were present in the HCAL barrel in 2022 (start of Run 3), before the TDC-based alignment method deployment. In particular, the pulse arrival time in depth 1 was ≈ 5 ns late, while the arrival in depths 3 and 4 at high $i\eta$ was up to 10 ns early. This position-dependent misalignment causes discrepancies in the time domain responses, as delayed signals appear prompt in some regions, while prompt signals appear delayed in other regions – and this cannot be well accounted for in the detector simulation. For accurate energy response, the prompt part of the HCAL signal must be integrated within the 25 ns timeslice, as the late part comes disproportionately from the low hadronic response. Additionally, a wide distribution of signal arrival times can increase jet energy resolution systematics due to the mismatch with simulation.

The wide-ranging effects of HCAL time alignment mean setting it as accurately as possible is vital. After the TDC-based alignment, the HB's energy resolution improved by about 10% due to mitigating arrival time differences across the HCAL depths.

3 Pulse Shape Effects

Before timing capabilities were introduced to the HCAL with the Phase-1 upgrade, the charge-weighted time (CWT) method was used to estimate the pulse timing from the energy distribution. CWT is defined by

$$\text{CWT} = \frac{\sum_i Q_i \cdot i \cdot 25 \text{ ns}}{\sum_i Q_i} \qquad i = 0...7 \qquad (1)$$

Q is the charge and i is the timeslice (8 total samples, each 25 ns, $i = 3$ as the SOI). Effectively, CWT measures the mean of the pulse energy, as illustrated in Figure 4.

CWT assumes pulse shapes are uniform across the whole detector and is thus biased by late fluctuations in the hadronic shower. CWT prioritizes maintaining a consistent SOI/(SOI+1) energy ratio (Q_3/Q_4) across the detector, as these are the two samples with the largest energy and thus most significant impact on the CWT result, at the loss of sensitivity to the position of the rising edge. However, with differing pulse shapes across HB, CWT leads

to inconsistent alignment. Depth 1 has lower CWT values due to a cleaner pulse shape and fewer late-time fluctuations, while depth 4 has higher CWT values due to more late-time contributions and an extended pulse shape. Thus, due to the depth-dependent non-linearity of CWT, selecting a set value of CWT results in a misalignment of the HCAL. In this case, when using CWT alignment, pulses in HB depth 1 arrive late, while depth 4 pulses arrive very early. This led to large alignment offsets within the detector before the implementation of TDC-based alignment in 2023.

TDC is a fundamentally accurate pulse time measure that does not assume a uniform pulse shape spanning multiple timeslices. As minimal timeslew is present above 4 GeV E_T, the rise time is an accurate measure of pulse arrival and is used for a new detector alignment method.
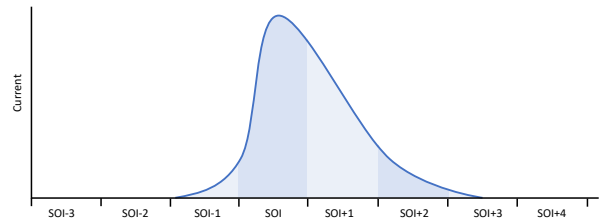

Figure 4. Illustration of the consecutive 25 ns timesamples CWT is derived from, with SOI containing the main part of the pulse.

3.1 Hadronic Shower Propagation

Depth 1 exhibits different behavior than the other depths, with a lower prompt fraction (65-70%, compared with 90-95% in all other depths) and a wider Gaussian evident in Figure 3. In addition, the delayed signal plateau (orange) is reached ≈ 3 ns later in depth 1 than in the other depths.

These differences in depth 1 are likely due to its placement directly behind the ECAL and lack of absorber material. Depth 1 is a very thin layer, made of only one scintillator layer: 9 mm of Bicron compared to four to six 3.7 mm thick layers of SCSN81 in all other depths. This scintillator is placed directly behind the ECAL support structures without a dedicated HCAL absorber layer (the ECAL support structure acts as an absorber layer). The thin depth 1 leads to a cleaner pulse shape, while the shower propagation through significant material before depths 3 and 4 (particularly at high $i\eta$) leads to a pulse shape with larger tails. Due to 5.8 λ_I in the HB (at $\eta = 0$, and increasing for larger η), depths 3 and 4 tend to have more hadronic shower fluctuations. The alternating layers of absorber and scintillator comprising each HCAL depth layer are illustrated in Figure 5.

3.2 Refinement of Charge Weighted Time

The high precision of TDC is used to refine CWT as an alternative time estimator. From the timing scan analysis presented in Section 2.2, the time alignment is well-known from the precision TDC data. However, the calculated
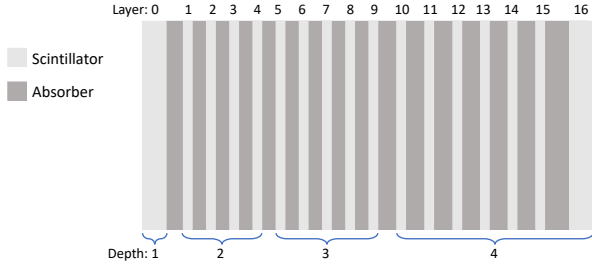
Figure 5. Diagram of the HCAL barrel scintillator and absorbers, indicating what comprises each depth layer. Depth 1 spans 177-190 cm, depth 2 190-214 cm, depth 3 214-245 cm, and depth 4 245-295 cm. The first and last absorbers are stainless steel, while all others are brass.

CWT values differ due to the differing pulse shapes across the detector. This section provides a method to reweight and calibrate the CWT method to account for the differing pulse shapes. This method may be used when precision timing information is unavailable as another handle for calorimeter time alignment.

3.3 Reweighting and Calibration Procedure

A reweighting and calibration procedure is derived to correct for the pulse shape effects in CWT. First, the pulse shape used to calculate CWT is reweighted. A vector of weight factors, $w_{i,depth}$ (depth and timeslice dependent), is introduced into CWT:

$$\text{CWT}_{\text{depth}} = \frac{\sum_i Q_i \cdot i \cdot 25 \cdot w_{i,depth}}{\sum_i Q_i \cdot w_{i,depth}} \qquad (2)$$

$$\text{with } i = 0...7 \text{ and depth} = 1...4$$

$w_{i=2,depth}$ and $w_{i=4,depth}$ (SOI-1 and SOI+1) are determined from (SOI-1)/SOI and (SOI+1)/SOI, and all other weights are 1, resulting in:

$$w_{i,depth} = \Big[1, 1, w_{i=2,depth}, 1, w_{i=4,depth}, 1, 1, 1\Big] \qquad (3)$$

$$w_{i=2,depth} = \frac{\text{ideal}(i=2)}{\frac{SOI-1}{SOI}} \qquad (4)$$

$$w_{i=4,depth} = \frac{\text{ideal}(i=4)}{\frac{SOI+1}{SOI}} \qquad (5)$$

where ideal($i = 2$) and ideal($i = 4$) are the selected ideal charge ratios between (SOI-1)/SOI and (SOI+1)/SOI, respectively, when the detector is aligned well. Deriving the weights based on (SOI±1)/SOI ratios normalizes pulse shapes to be uniform across depths, aligning with the CWT assumptions.

After reweighting, a calibration (slope correction) is applied. When CWT is plotted against the phase setting, some regions exhibit non-linear behavior. Focusing on the central region (-4 to 8 ns), the calibration provides a method to achieve linearity in phase change and CWT response. The correction factors are determined from a linear fit to $\text{CWT}_{\text{depth}}$, giving the slope and intercept m_{depth}

and b_{depth}. The calibrated CWT is:

$$\text{Calibrated CWT}_{\text{depth}} =$$

$$\frac{1}{m_{\text{depth}}} \cdot \text{CWT}_{\text{depth}} + b_{\text{depth}} \left(1 - \frac{1}{m_{\text{depth}}}\right) \quad (6)$$

CWT is now linear in phase delay, as pulse shape effects have been accounted for. The reweighting and linearization procedure improves CWT's capabilities as a timing variable, preventing timing misalignments by several ns that can occur if the pulse shape differences between depths and $i\eta$ are not accounted for. Reweighting accounts for pulse shape effects, and linearization calibrates CWT to give the expected response to a change in alignment phase setting.

4 Conclusions

Calorimeter timing information has been used to develop and implement a new time alignment procedure for the CMS experiment's hadron calorimeter. Alignment to within 0.5 ns has improved detector performance and energy resolution. The hadron calorimeter's new timing and segmentation capabilities are also utilized in a novel timing trigger, with the implementation described in [5] and the trigger performance detailed in [6].

An additional alignment method based on reweighted pulse shape distributions is refined and calibrated with the higher precision TDC to correct for the pulse shape dependence of CWT. The pulse shape timing method provides additional avenues for calorimeter timing, such as corrections when a clock scan cannot be done, or for use in software triggering and pulse reconstruction.

References

[1] CMS Collaboration, *CMS Technical Design Report for the Phase 1 Upgrade of the Hadron Calorimeter*. CMS-LHCC-2012-015, 26 September 2012. https://cds.cern.ch/record/1481837/files/CMS-TDR-010.pdf

[2] T. Roy et. al, *QIE: performance studies of the next generation charge integrator*. 2015 JINST **10** C02009 DOI 10.1088/1748-0221/10/02/C02009

[3] CMS HCAL Collaboration, *HCAL uTCA Trigger and Readout Module (uHTR)*. CMS Public DocDB, 23 July 2020. https://cms-docdb.cern.ch/cgi-bin/PublicDocDB/RetrieveFile?docid=12306&filename=uhtr_spec.pdf&version=21

[4] CMS Collaboration, *Performance of long-lived particle triggers in Run 3*. CERN CMS DP-2023/043, July 2023. http://cds.cern.ch/record/2891496?ln=en

[5] Gillian Kopp, et. al, *Design of a Long-lived Particle Trigger with the CMS Hadron Calorimeter*. LHCP2024, 3-8 June 2024. Conference Proceedings [in preparation]. https://indico.cern.ch/event/1253590/contributions/5849234/

[6] Gillian Kopp, on behalf of the CMS Collaboration, *Long-lived Particle Trigger Capabilities of the CMS Hadron Calorimeter*. ICHEP2024, 17-24 July 2024. Conference Proceedings [in preparation]. https://indico.cern.ch/event/1291157/contributions/5878371/